Supporting Information

In-depth Chiral Sensing Capability of C-Dots in Biomimetic Protein-Based Hydrogel: A Probe for Chiral Recognition Applications

Sapna Waghmare, [a] Umarfaruk S. Sayyad,[a] Arunavo Chatterjee,[b] Somen Mondal[a]*

a. Institute of Chemical Technology, Mumbai, Marathwada Campus, Jalna, Maharashtra 431203, India

b. Indian Institute of Science Education and Research Kolkata, Mohanpur 741246 WB, India

Corresponding Author: Dr. Somen Mondal, E-mail: s.mondal@marj.ictmumbai.edu.in*

1. Experimental section:

1.2 Materials:

Citric acid was obtained from Sigma Aldrich, while D/L-cysteine hydrochloride was sourced from MERCK. Analytical-grade acetone, ethanol, and methanol were acquired from Molychem. Sulfuric acid was procured from Avra Chemicals, and sodium chloride was obtained from SDFCL. Bovine serum albumin (BSA) was purchased from MP Biomedicals. FTO glass was sourced from Global Nanotech. All chemicals had a purity of over 99%, and all experiments were performed using Milli-Q water.

1. 2. Method:

1.2. 1. Synthesis of Chiral Carbon Dots:

The chiral C-Dots were synthesized using a microwave irradiation method, with citric acid serving as the carbon source and D/L-cysteine hydrochloride as the chiral ligand, following a previously reported procedure.[1-3] First, 100 mg of citric acid and 98 mg of D/L-cysteine hydrochloride were dissolved in 3 mL of deionized water and sonicated for 30 minutes to obtain a clear solution. The reaction mixture was then placed in a vial and subjected to microwave irradiation at 180°C, with a power of 150 W and a pressure of 250 psi, for 30 minutes in dynamic mode. Upon completion of the reaction, the mixture changed to a dark brown color. The solvent was then evaporated using a rotary evaporator at 60°C. The resulting gel was sequentially washed with acetone, methanol, and a 1:1 mixture of acetone and methanol. Finally, the synthesized carbon dots (C-Dots) were

dissolved in deionized water for further characterization and application studies. The chirality in the C-Dots was derived from the chiral ligands; thus, C-Dots synthesized using D-cysteine and L-cysteine were named D-C-Dot and L-C-Dot, respectively. In contrast, the achiral C-Dots synthesized from a 1:1 mixture of chiral ligands (D-cysteine and L-cysteine) are referred to as a racemic mixture. Moreover, we have synthesized achiral C-Dots using only citric acid with any coating agent. Due to the presence of equal and opposite spins in the core state of the C-Dots, the overall spin becomes zero, resulting in the absence of chirality, thus categorizing them as achiral C-Dots.

1.2.2 Synthesis of BSA Hydrogel Gel (B-Gel): B-Gel was synthesized following the previously reported literature.[4] The BSA protein powder was dissolved with the desired weight concentration (w/v) in 75 mM NaCl at pH 2. The solution was then poured into a petri dish and heated at 75°-80°C for approximately 8 hours.[4] Finally, the BSA solution was converted into B-Gel through the gelation process.

1.2.3. Synthesis of Chiral and Achiral B-Gel: Chiral C-Dots, including D-C-Dots and L-C-Dots, as well as achiral carbon dots (A-C-Dots), were added to a prepared BSA solution containing 75 mM NaCl at pH 2. The resulting C-Dots solution (D-C-Dots, L-C-Dots, and A-C-Dots) was then poured into a petri dish and heated at 75–80°C for approximately eight hours. This process led to the formation of chiral gels (D-Gel and L-Gel) and an achiral gel (A-Gel) from the C-Dots-doped BSA solution. Specifically, the chiral gels were synthesized from D-C-Dots and L-C-Dots, while the achiral gel was synthesized using A-C-Dots, which is why it is called D-Gel, L-Gel, and A-Gel, respectively.

1.2.4. Electrode fabrication: The fluorine-doped tin oxide (FTO) coated glass pieces were sequentially cleaned using deionized (DI) water, ethanol, and acetone for 15 minutes each. After cleaning, the FTO glass was dried and placed 1 cm x 1 cm gel samples on the conducting side of an etched FTO for electrical study. Unbounded water of gel was removed using tissue paper and used it for further electrochemical studies.

1.2.5. Sensing application: Chiral sensing was performed using an electrochemical workstation with a two-electrode system. Initially, the D/L-Gel composite was placed onto an etched FTO electrode, followed by the dropwise addition of chiral D/L-cysteine and other chiral ligands.

Further, we waited few minutes to reach the system in equilibrium and measured the current density by LSV measurements.

2. Instrumentation and Characterization:

2.1. Transmission Electron Microscopy (TEM) and High-Resolution TEM (HRTEM):

The particle size and surface morphology of C-Dots were examined using a JEOL JEM-2100F microscope at an accelerating voltage of 200 keV. For TEM analysis, the C-Dots were diluted and deposited onto a carbon-coated copper grid, then stored in a vacuum desiccator for 12 hours. After drying, the grids were utilized to capture TEM images.

2.2. Fourier Transform Infrared Spectroscopy (FTIR):

The surface functional groups of C-Dots and B-Gel were analyzed using a JASCO FT/IR 6600 spectrometer in ATR mode at room temperature.

2.3. UV-Visible and Photoluminescence (PL) Spectroscopy:

UV-Visible and Photoluminescence (PL) Spectroscopy:

The steady-state absorbance of the samples was recorded using an LMSP-UV1900 UV-Vis spectrophotometer, while their steady-state fluorescence was measured with HORIBA FLUROMAX PLUS P-0924G-1425-FMPLUS.

2.4. Time-Correlated Single Photon Counting (TCSPC) Measurement:

Fluorescence decay measurements were conducted using a HORIBA Scientific Delta Pro-DD TCSPC lifetime system, featuring a pulsed 340 nm Nano-LED excitation source and a 400 nm long pass filter. The fluorescence decays were analyzed with EZ Time software, and the system had an instrument response function (IRF) of 1.2 ns.

2.5. Circular Dichroism (CD) Spectroscopy:

Chirality of C-Dots and C-Dots-B-Gel were performed using a Jasco J-815 Circular Dichroism spectrophotometer.

2.6. Electrochemical Measurements:

All electrical measurements were conducted using a Metrohm Autolab electrochemical workstation with fabricated electrodes in a two-electrode system. Electrochemical impedance measurements were performed over a frequency range of 1 Hz to 1 MHz. Chronoamperometry and voltametric current measurements were carried out at an applied potential of +0.5 V. Photocurrent generation was evaluated under UV-light irradiation using photo reactor. The data acquired were analyzed using Nova 2.1 software, as recommended by Metrohm.

2.7. Fluorescence Lifetime Imaging Microscopy (FLIM):

The FLIM images were obtained by a confocal laser scanning microscope (Axio Observer A1) from Zeiss coupled with a DCS-120 system from Becker & Hickl (BH) GmbH for fluorescence lifetime imaging and a picosecond diode laser (BDL-405-SMC, BH) with λ_{ex} = 405 nm. The scanning was controlled by a BH GVD-120 scan controller. The BH HPM-100-40 hybrid detector module in the DCS120 system was controlled by DCC-100 software. A long-pass filter (HQ495LP) was placed to block the excitation light and also to monitor the emission. The TCSPC FLIM system is controlled by the "SPCM" TCSPC operating software and the DCC-100 detector controller software. The emitted light from a selected point of the sample was collected by the microscope lens, scanned by the galvanometer mirrors, separated from the excitation beam, split into two channels of different wavelengths, and focused into pinholes in a plane conjugated with the focal plane in the sample. The out of focus light was thus suppressed. The FLIM images were analyzed in SPC-Image software for decay measurement at a particular point of the sample. For FLIM studies, the microscope glass slides were cleaned thoroughly by sequential washing in an ultrasonic bath with water, alcohol, acid, and alkali and dried properly. A selected portion of each of freshly prepared BSA-hydrogel gel (both doped and non-doped) were put on the glass slides and were scanned for the FLIM microscopy.

2.8. Formula for Stern-Volmer Constant:

Extent of quenching was calculated using the Stern-Volmer equation:

$$\frac{F_0}{F} = 1 + K_{sv}C_q$$

where F_0 and F are the PL intensities of the chiral C/D-Gel on adding the chiral D and L Cys in the absence and presence of quencher. K_{sv} is the Stern-Volmer quenching constant, C_q is the concentration of the quencher.

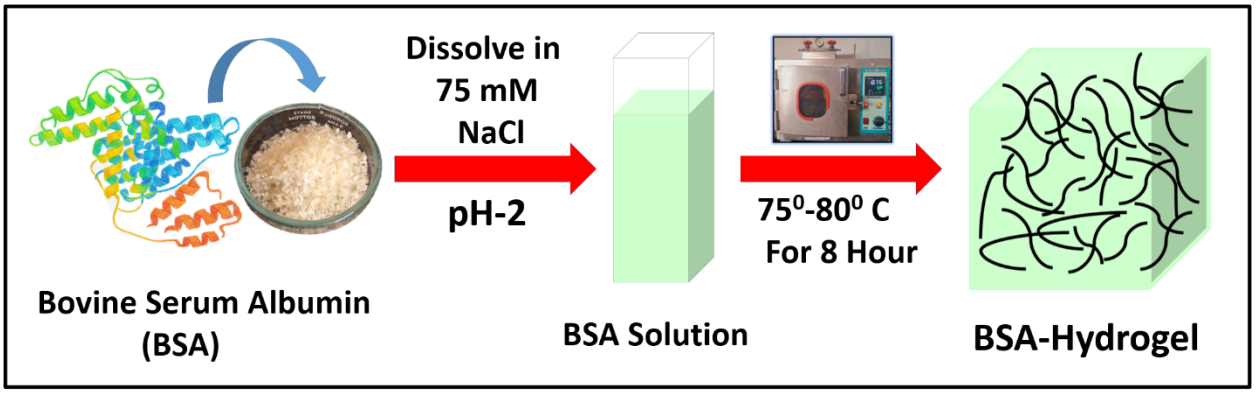

Figure S1: Schematic representation of synthesis steps of B-Gel composite

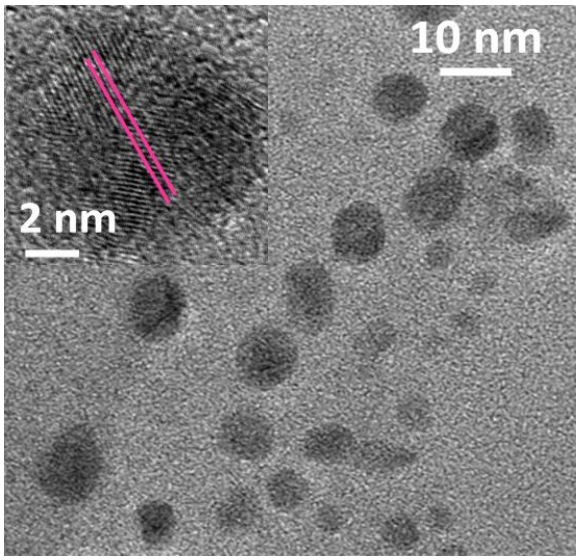

Figure S2: TEM image of A-C-Dot

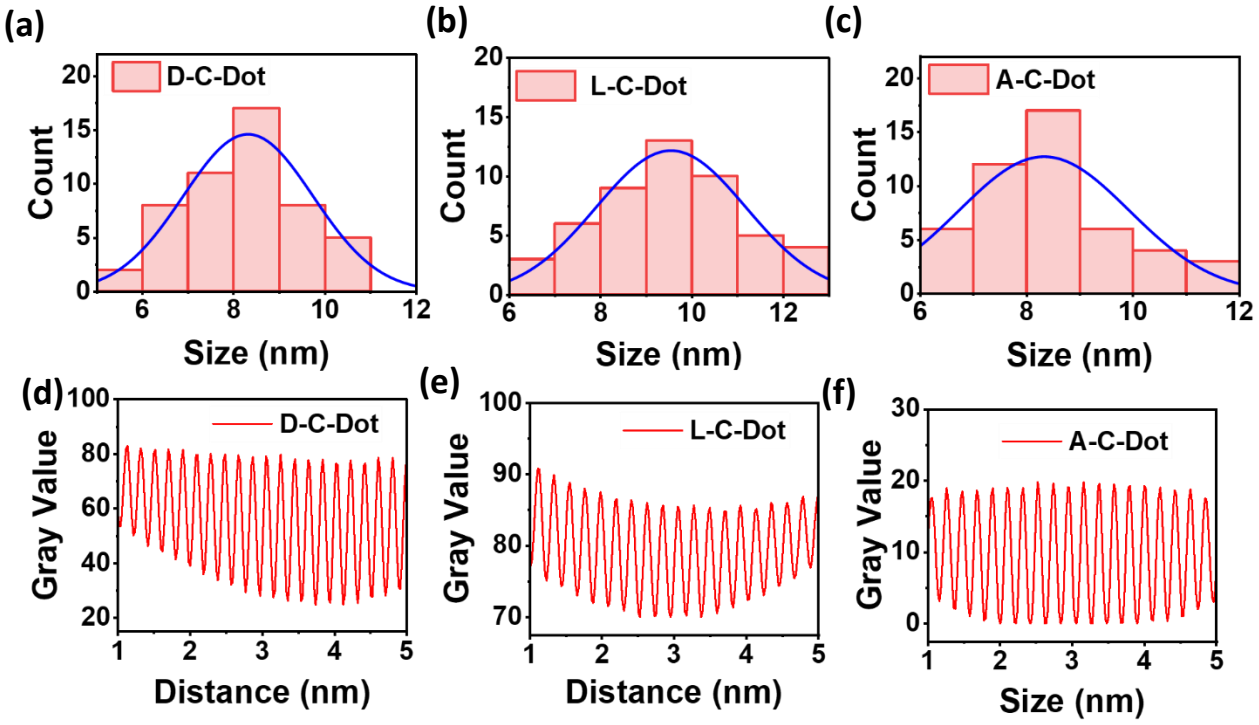

Figure S3: Size distribution histogram spectra of chiral (a) D-C-Dot (b) L-C-Dot (c) A-C-Dot and line profile of (d) D-C-Dot (e) L-C-Dot (f) A-C-Dot

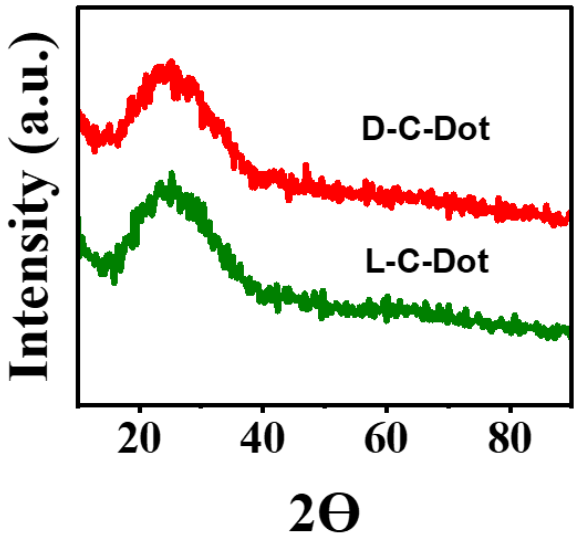

Figure S4: XRD spectra of chiral D/L-C-Dot

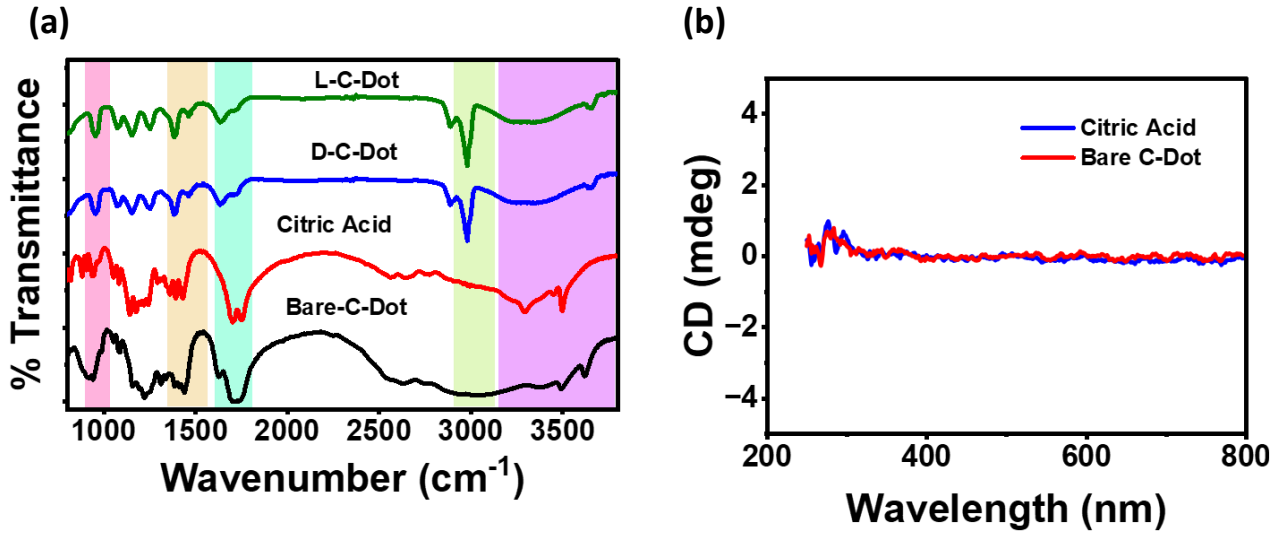

Figure S5: (a) FTIR spectra of chiral C-Dots aping with chiral ligand, citric acid and bear-C-Dots without capping ligands (b) CD spectra of citric acid and bear C-Dots.

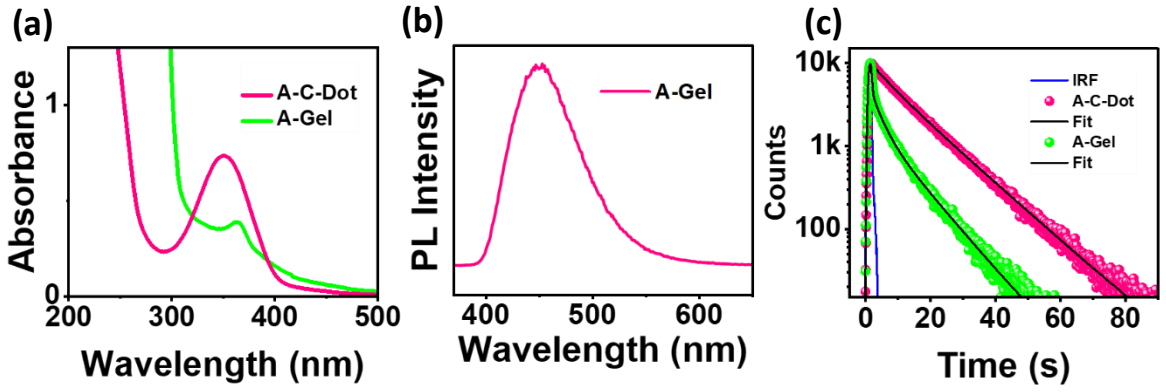

Figure S6: (a) UV-Vis Absorbance spectra of A-C-Dot and A-Gel (b) PL spectra of A-Gel (c) PL decay of measurement of A-C-Dot and A-Gel.

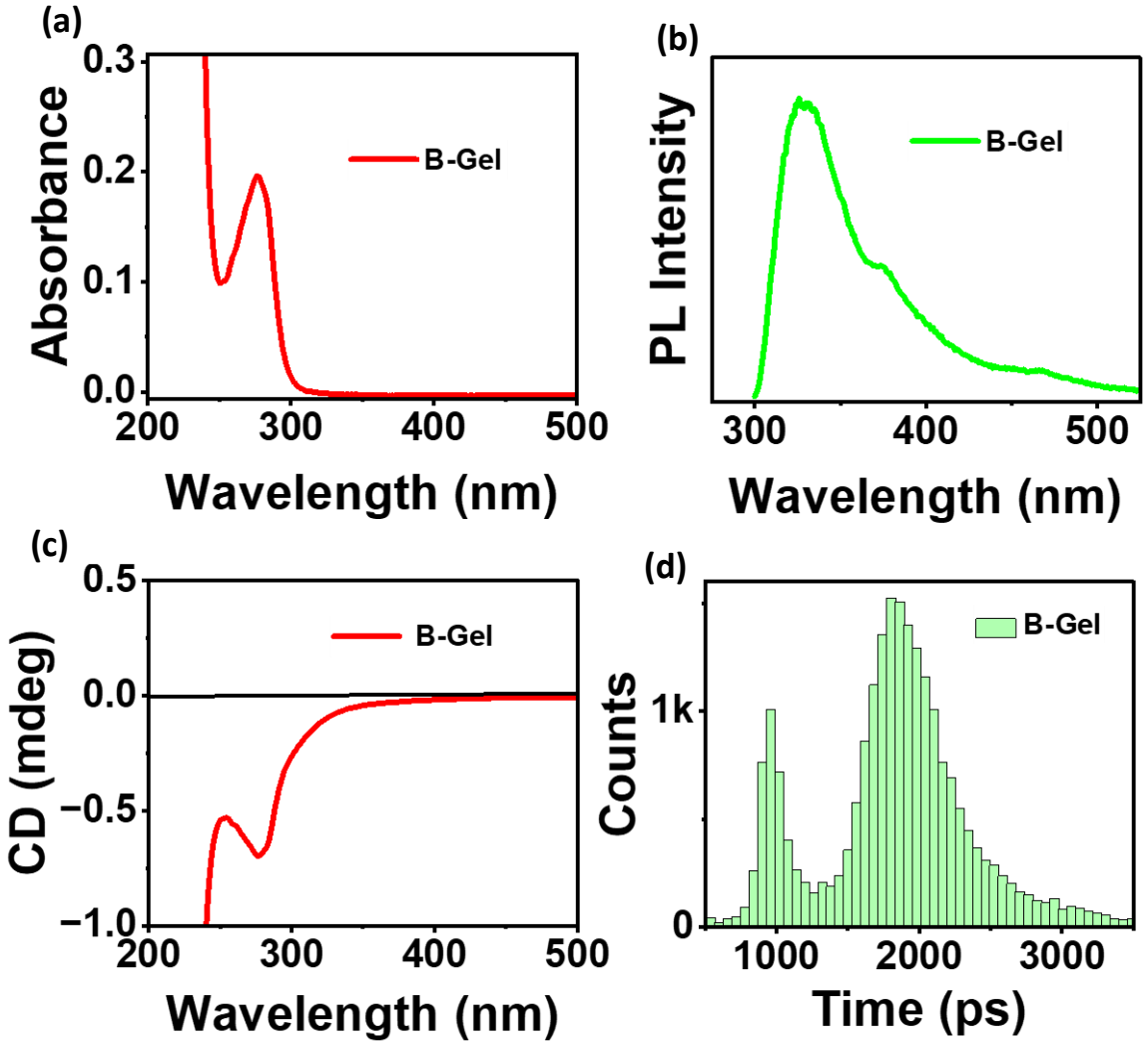

Figure S7: (a) Absorbance spectra of B-Gel (b) PL Spectra of B-Gel (c) CD measurement of BSA-Gel (d) histogram of PL lifetime distribution of B-Gel was measured by FLIM.

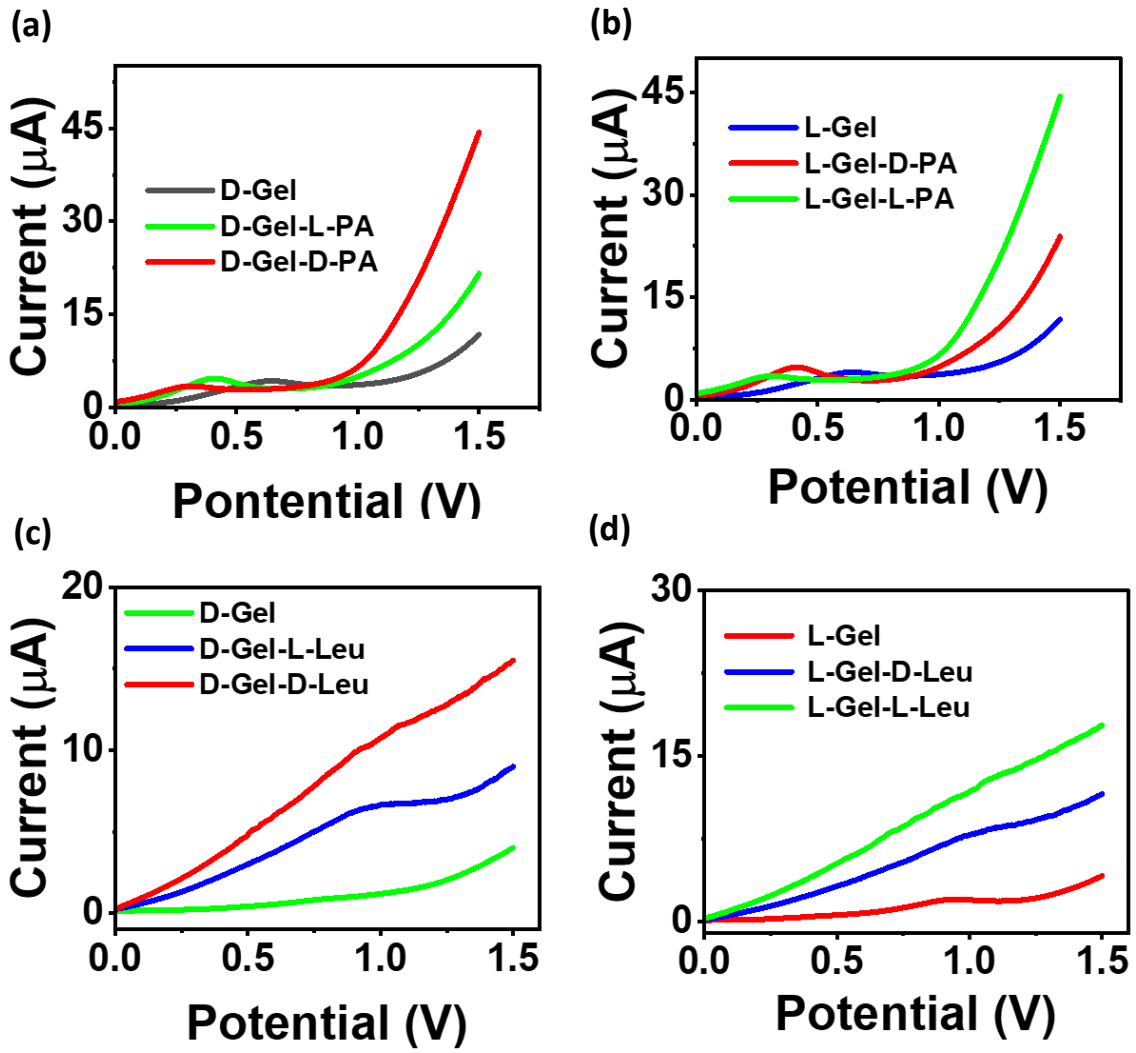

Figure S8: LSV measurement of (a) D-Gel with D/L Lue (b) L-Gel with D/L Lue (c) D-Gel with D/L PA (d) L-Gel with D/L PA

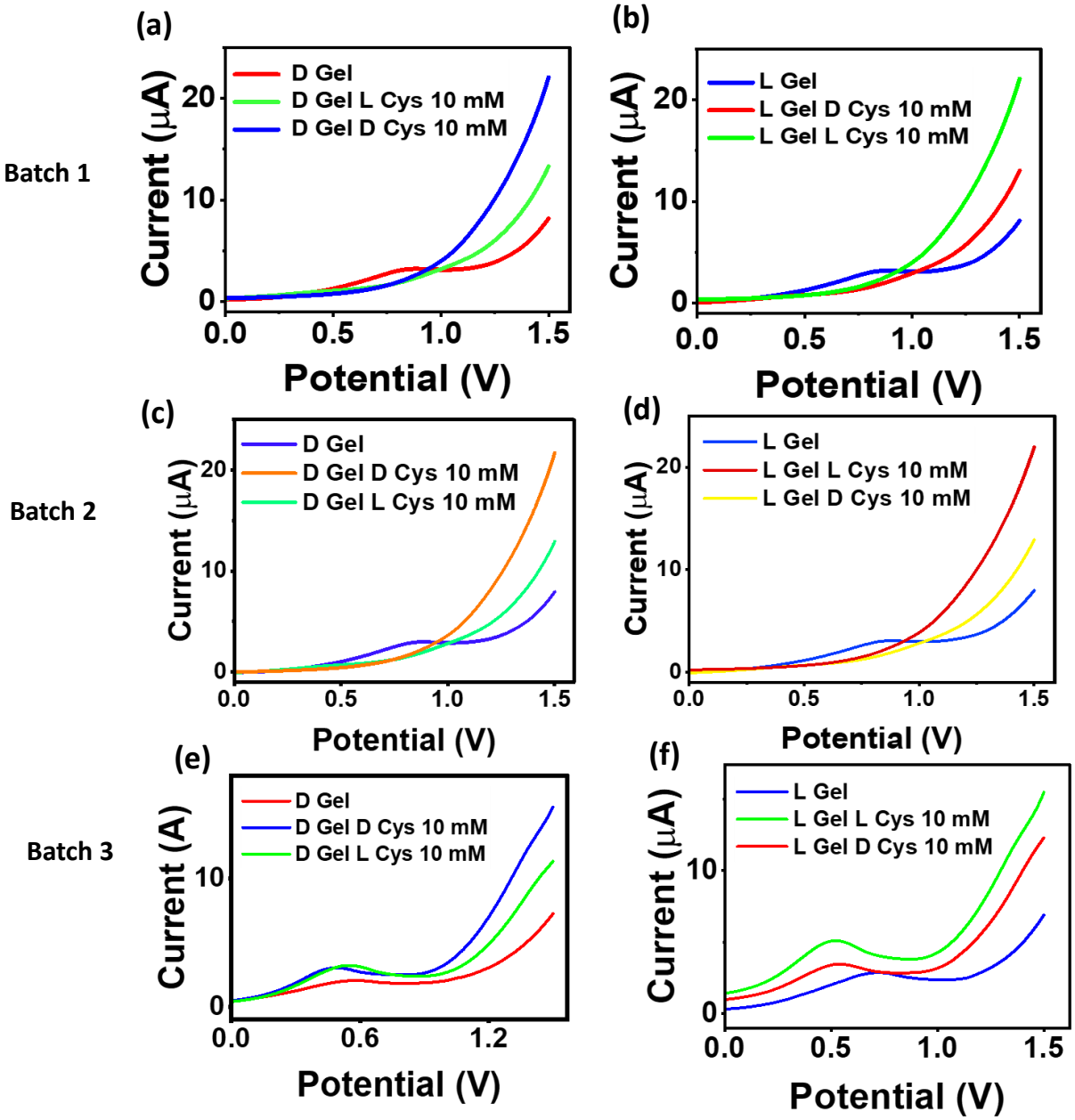

Figure S9: LSV spectra of three different batches of gel (a, c, e) D-Gel with D and L Cys (b, d, f) L-Gel with D and L Cys

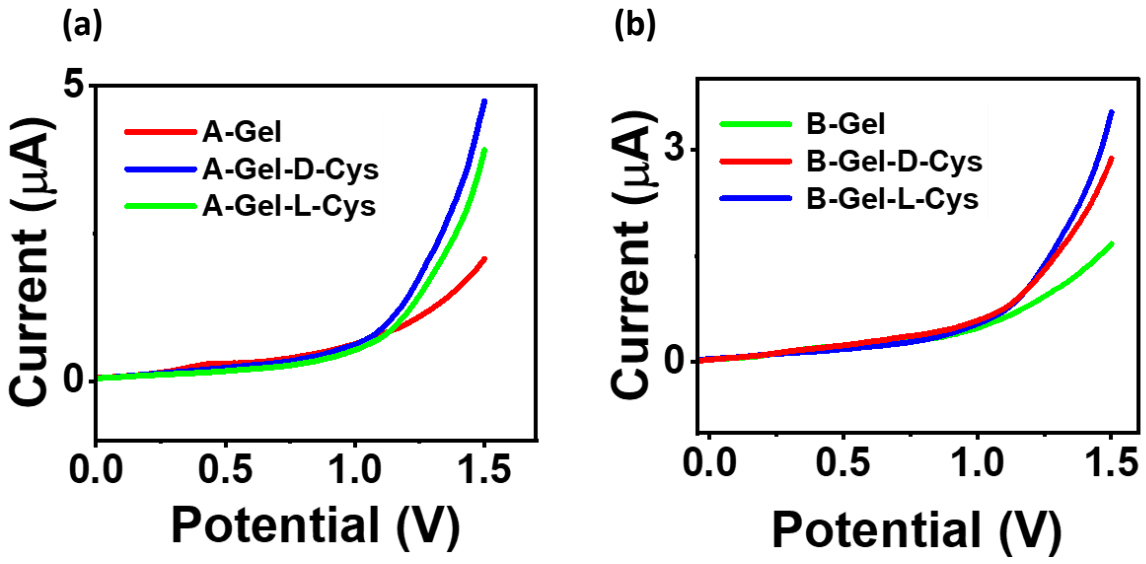

Figure S10: LSV spectra of (a) A-Gel with D/L Cys (b) B-Gel with D/L Cys

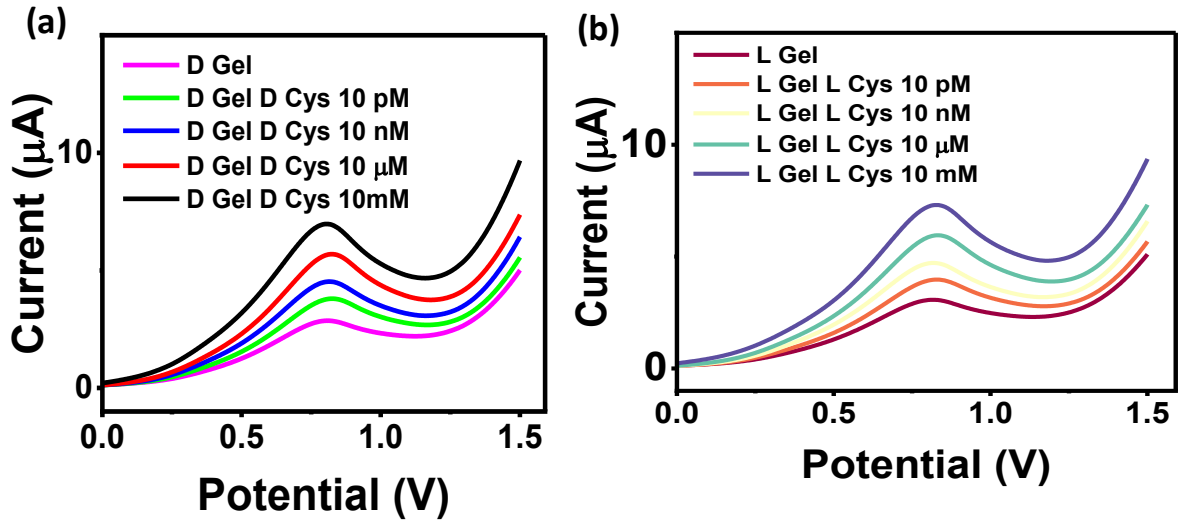

Figure S11: LSV spectra of (a) D Gel with D-Cys (b) L Gel with L-Cys with different concention from 10 pm to 10 mM

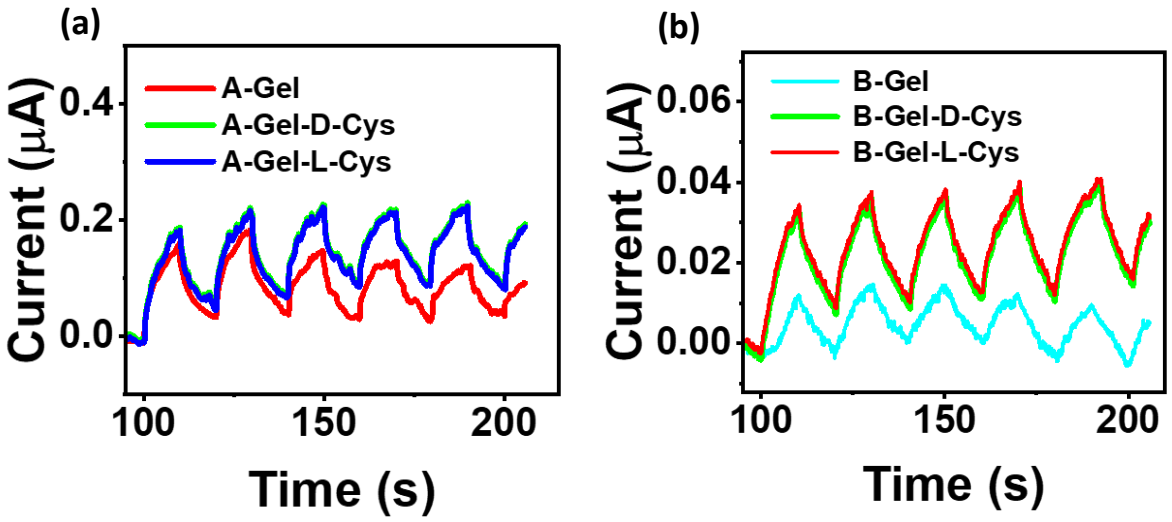

Figure S12: Transient photocurrent was measured in (a) A-Gel with D/L Cys (b) B-Gel with D/L Cys

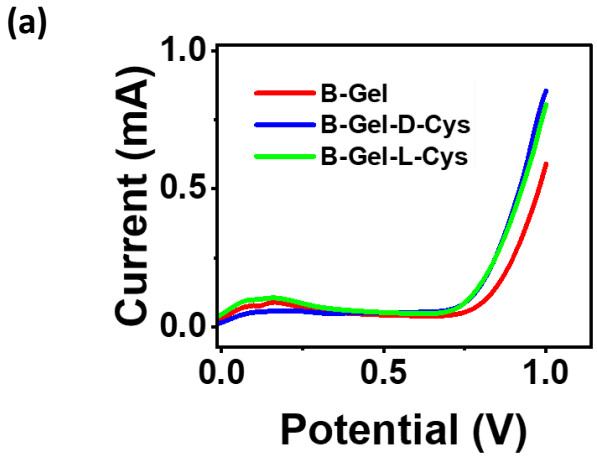

Figure S13: In depth LSV measurement in B-Gel with the addition of D-Cys and L-Cys

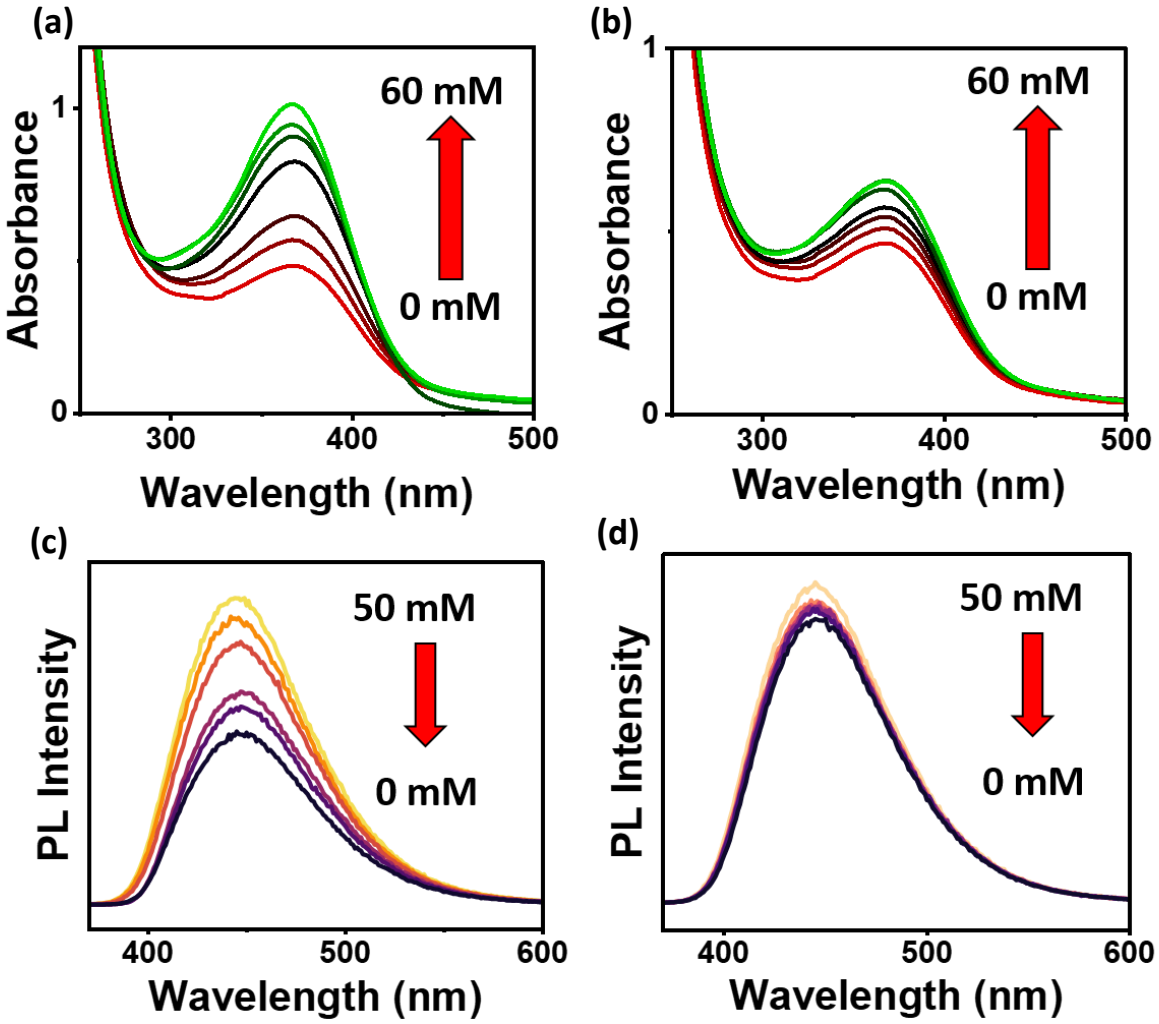

Figure S14: (a) UV interaction Spectra of (a) L-Gel with L-Cys (b) L-Gel with D-Cys, PL spectra of (c) L-Gel with L-Cys (d) L-Gel with D-Cys

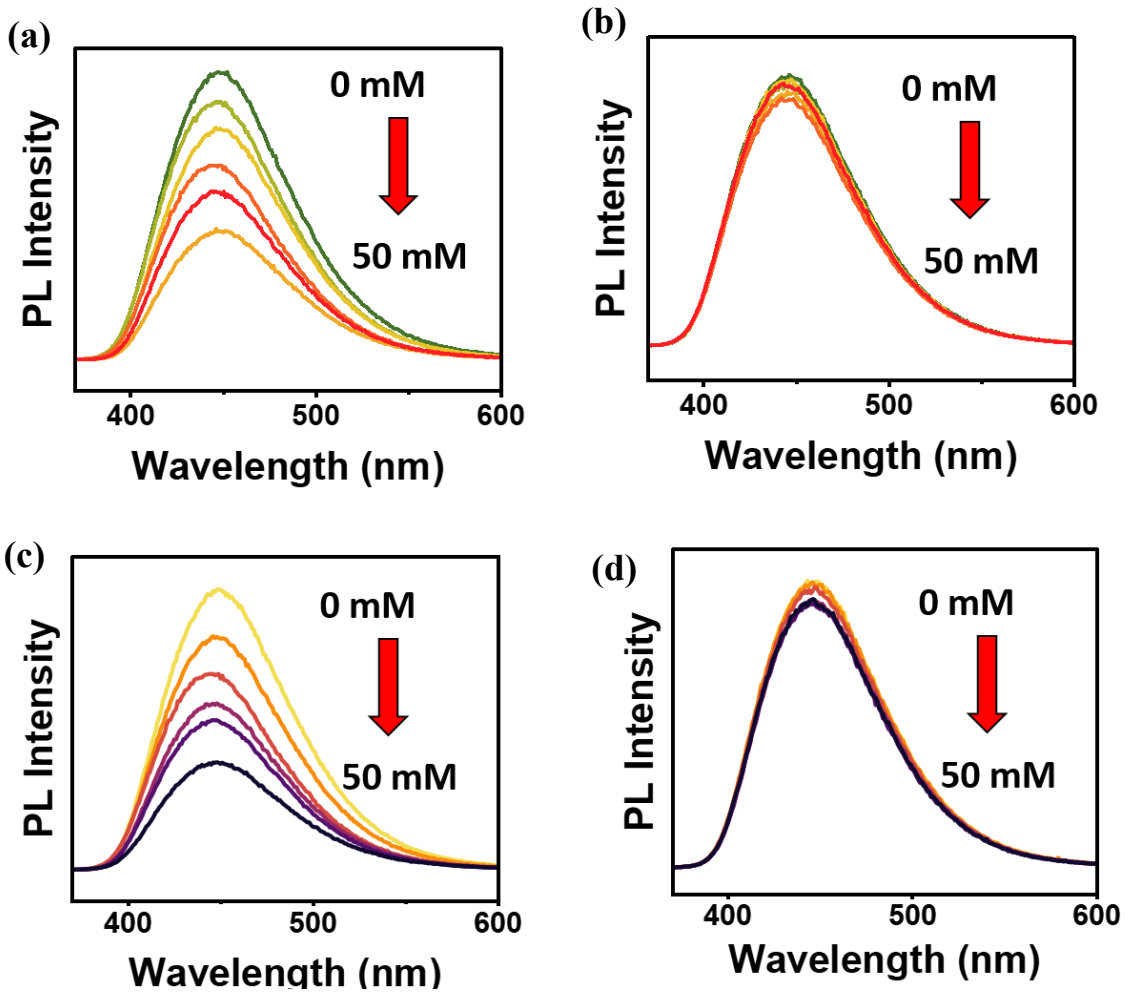

Figure S15: PL Spectra of (a) D-Gel with D-Leu (b) D-Gel with L-Leu (c) D-Gel with D-PA (d) D-Gel with D-PA

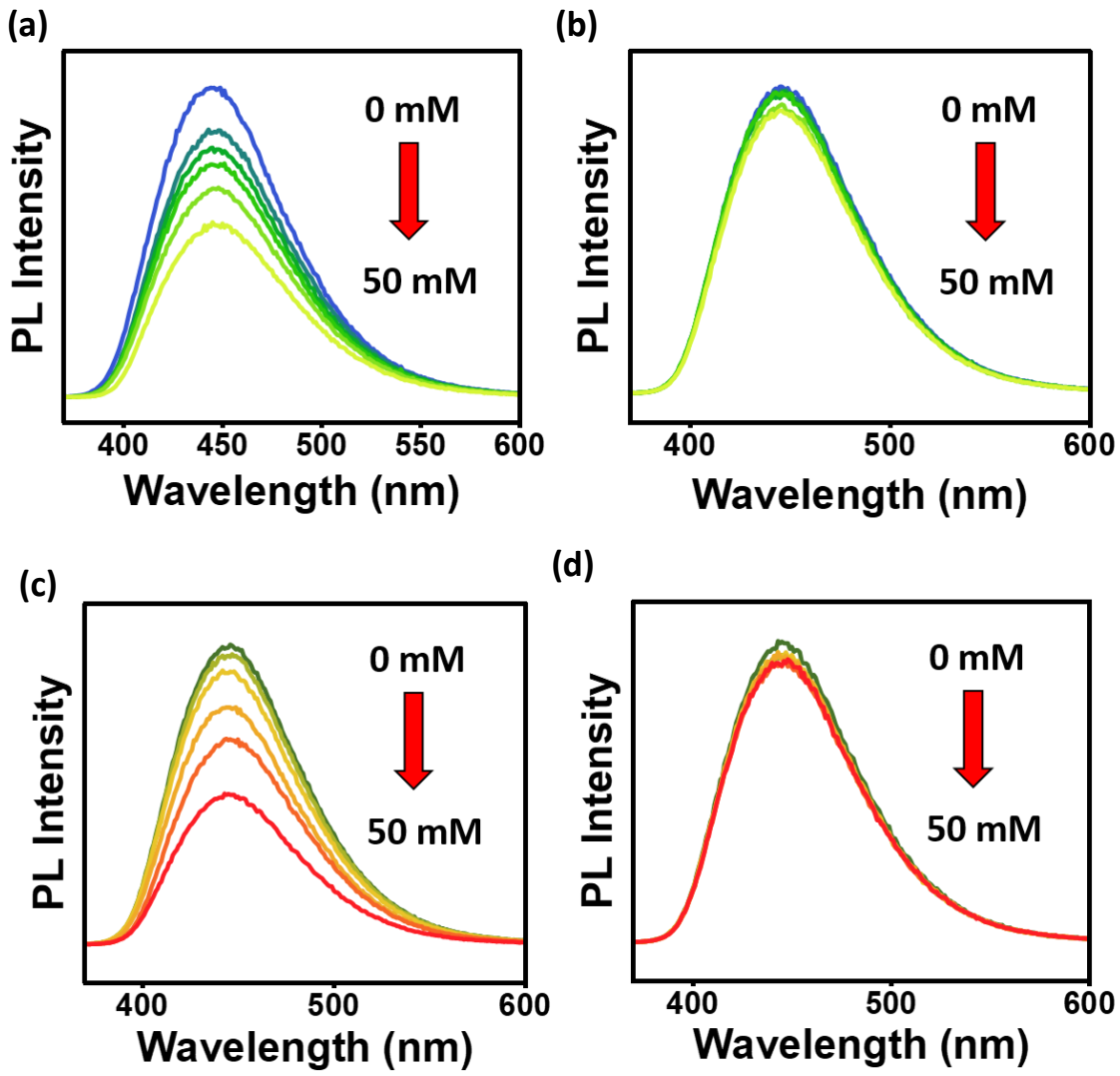

Figure S16: PL Spectra of (a) L-Gel with L-Leu (b) L-Gel with D-Leu and (c) L-Gel with L-PA (d) L-Gel with D-PA

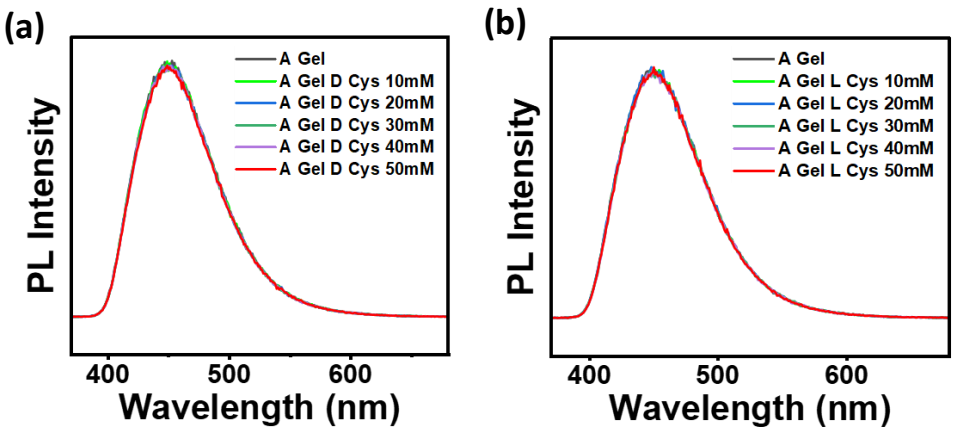

Figure S17: PL Spectra of (a) A-Gel with D-Cys (b) A-Gel with L-Cys

Table S1: Fitting time constants of all C-Dots were calculated by time-resolved fluorescence measurement.

System	τ_1 (ns)	B_1 (%)	χ^2
D-C-Dot	11.0592	100	2.1
L-C-Dot	11.0759	100	2
A-C-Dot	10.9626	100	1.8

Table S2: Fitting time constants of all C-Dot-Gel composite systems were calculated by time-resolved fluorescence measurement.

System	τ_1 (ns)	B_1 (%)	τ_2 (ns)	B_2 (%)	τ_3 (ns)	B_3 (%)	χ^2	$<\tau>$ (ns)
D-Gel	0.151	27.1	2.88	24.01	9.49	48.89	1	5.37
L-Gel	0.180	30.24	2.93	22.3	9.63	47.47	1	5.28
A-Gel	0.155	27.12	2.93	24.64	9.48	48.24	1.1	5.34

Table S3: Conductivity of B-Gel and chiral C-Dots-B-Gel Composite system

System	L (mm)	R (Ohm)	W (cm)	T (mm)	Conductivity ($S.cm^{-1}$)
B-Gel	0.5	1413403	1	0.04	0.89×10^{-5}
D-Gel	0.5	419492	1	0.04	2.97×10^{-5}
L-Gel	0.5	369041	1	0.04	3.38×10^{-5}
A-Gel	0.5	1229436	1	0.04	1.01×10^{-5}

Table S4: Comparison of conductivity of BSA composite hydrogels in specific condition

System	Conductivity ($S.cm^{-1}$)	Condition	References
B-Gel	0.89×10^{-5}	ambident	Our work
D-Gel	2.97×10^{-5}	ambident	Our work
L-Gel	3.38×10^{-5}	ambident	Our work
A-Gel	1.01×10^{-5}	ambident	Our work
BSA−Nafion 117	0.3	80°C and 95 %	5
BSA-GO	4.7	-	6

References:

(1) S. Burai, S. Waghmare, A. Chatterjee, P. Purkayastha, S. Mondal, S, *J. PhyS. Chem. C* **2023,** *127*, 11730-11735.

(2) S. Waghmare, U. S. Sayyad, A. Chatterjee, P. Purkayastha, S. Mondal, S. *J. Phys. Chem. C* **2024,** *128*, 9345-9352.

(3) S. Waghmare, U. S. Sayyad, A. Chatterjee, S. Mondal, *J.Phys.Chem. L* **2024,** *15*, 11275-11281.

(4) N. Amdursky, M. M. Mazo, M. R. Thomas, E. J. Humphrey, J. L. Puetzer, J. P. St-Pierre, S. C. Skaalure, R. M. Richardson, C. M. Terracciano, M. M.Stevens, M. M., *J.Mater.Chem. B* **2018,** *6*, 5604-5612.

5. W. Jia, P. Wu, *ACS Appl. Mater. Interfaces* **2018**, 10, 46, 39768–39776.

6. S. Garg, S. Tripathi, S. Agrawal, V. Tiwari, A. S. Parmar, C*olloids and Surfaces A: Physicochemical and Engineering Aspects* **2025**, 705, 135553.